Hindawi
Advances in Civil Engineering
Volume 2020, Article ID 8810079, 12 pages
https://doi.org/10.1155/2020/8810079

Research Article

Effect of Admixture on the Hydraulic Conductivity of Compacted Loess: A Case Study

Pan Liu, Xuejiao Zhang, Min Zhang, and Xueqiang Yang

School of Civil and Transportation Engineering, Guangdong University of Technology, Guangzhou 510006, China

Correspondence should be addressed to Xueqiang Yang; xqyfls@126.com

Received 29 April 2020; Revised 7 June 2020; Accepted 29 August 2020; Published 10 September 2020

Academic Editor: Yixian Wang

Hydraulic characteristic of the exposed ground plays an important role in the construction of "sponge city," which is a popular concept in the world recently. Loess soil, which is a common geomaterial in its distribution area approximately 9.3% of the world's land surface, usually could not satisfy the engineering requirement only by compacting without any other treatments. This paper aims to investigate the effect of a natural geomaterial, lateritic soil, which is more economical and environmental than the traditional admixtures such as cement and lime, on the saturated hydraulic conductivity (k_{sat}) of compacted loess. A series of falling-head permeability tests on pure loess and lime-treated loess were carried out firstly for comparison; then lime-treated loess mixed with different contents of lateritic soil was tested. To verify the availability of the coverage of high density lateritic soil on pure loess for antipermeability, which is a common treatment in local area, tests of different thickness of the coverage were conducted. The test results revealed that the admixture of lime could obviously decrease k_{sat} of pure loess and 3% might be the most economical content. An empirical algorithm was proposed based on the results to estimate k_{sat} of lime-treated loess of which the lime content is out of the scope studied in this paper, and it would be useful for engineering design and numerical simulation of safety evaluation. The addition of lateritic soil in the 3% lime-treated loess could further decrease k_{sat} and its performance for antipermeability was better than increasing the lime contents simply. The coverage of high density lateritic soil could also improve the antipermeability of loess, and thickness at least of 30 mm was suggested for engineering practice.

1. Introduction

Loess, a typical eolian deposit, is abundant in central Asia, Europe, northern America, southern Africa, and especially northwestern China [1–5]. The area of loess land is 13 million square kilometers, about 9.3% of the whole land area in the world. Loess is the most common geomaterial in these areas. In its natural state, the soil has a low dry density, a large void ratio, and a metastable soil structure which would collapse rapidly during wetting [6–10]. This wetting-induced collapse behavior has resulted in many engineering problems. For example, in heavy rainstorm conditions, nonuniform deformation of many pavements takes place as a result of the large hydraulic conductivity of substrate filled by recompacted loess, which allows large amounts of water to infiltrate the natural loess below [11–13]. The local recompacted loess cannot satisfy the engineering requirements because of its high hydraulic conductivity. So, in this situation, soil treatment becomes essential to improve the engineering properties of the local soil [14–17].

Currently, the additions of cement and lime into compacted loess are the most common treatments in engineering practice, and the effect of cement and/or lime content on the mechanical behavior of the treated loess has been reported frequently [18–20]. The chemical reaction of cement or lime would result in aggregates forming as bonding among the soil particles, which would enhance the strength of the soil. The pore size distribution would also be changed, the macropores decrease, and the micropores increase, which may cause the change of hydraulic conductivity [21]. Gao et al. [22] conducted a series of hydraulic tests on lime-treated loess with different dry densities and lime contents and proposed the fact that the lime content of 9% and the compaction degree of 95% should be used in

loess soil improvements at Yan'an city. The hydraulic conductivity of loess soils was also influenced by many other factors, e.g., temperature [23, 24]. However, the effect of other factors is out of the scope of this study.

The concept of "sponge city" is popular in China recently, and about 30 cities were involved into the experimental project funded by the government. Most cities in this project locate on the loess plateau in northwestern China, because of the fact that the soil erosion induced by rain water in these cities has been seriously resulting from the unsatisfied properties of the loess. The hydraulic conductivity of the exposed ground soil, which should be greatly improved, is an important characteristic for building a sponge system. However, both cement and lime are expensive, and their production is known to release a plenty of greenhouse gases that is causing environmental problems in our world [25, 26]. Consequently, it is an urgent need to find other materials which are more economical and environmental to replace cement and lime partially or totally and meantime to satisfy the engineering requirement. This paper aims to study the effect of lime content on the saturated hydraulic conductivity (k_{sat}) of a typical loess in China firstly, and furthermore a local natural geomaterial, lateritic soil, is added to the lime-treated loess before compacting to find out whether it can further decrease k_{sat} or not. Besides, local people used to cover the sunken loess ground with high density lateritic soil to make the rainwater be stored longer, and then alternative research is needed to find out the influence of the coverage on k_{sat} of the double soil structure; the falling-head permeability tests of different thickness of lateritic soil coverage were carried out in this study.

2. Soil Description

The loess used in this study was taken from an exploratory hole located in Qingyang, China (a city locates on the loess plateau and is trying to build a sponge system). The depth of loess sample was about 1.50 m below the ground, as seen in Figure 1 (location A). From visual inspection, the soil was mainly brown in color, with some yellowish-brown patches. The lateritic soil (LAT) sample was obtained from a natural slope, as shown in Figure 2. The straight-line distance between the locations of loess sample and LAT sample was about 2 km. The LAT soil was mainly red brown in color. The satellite imageries in the left component of Figures 1 and 2 are obtained from Baidu Map (https://map.baidu.com). The physical properties of the two soils were obtained according to the ASTM standards (ASTM, 2017) [27] and summarized in Table 1.

Their particle size distributions (PSDs) obtained by sieving and hydrometer analysis are shown in Figure 3. In order to verify the homogeneity of the loess soil in this city area, another two loess soils obtained from different locations (location B: N35°47′57.86″ E107°36′24.15″ and location C: N35°40′0.62″ E107°40′45.77″) with the same depth of 1.50 m were tested. For clarity, the PSD curves of the loess in locations B and C are illustrated by dark grey lines without data points in Figure 3. It can be seen that the three curves of loess from different locations are closed to each other, which means that the loess layer in this city area is highly homogeneous, as it should be expected. The silt fraction is dominant in both loess and LAT, and the LAT has more contents of clay than those of loess (Table 1). Figure 4 shows the PSD curve of the loess in this study, with PSD curves of some other loess soils in the previous study for comparison. The curve of the loess in this study lies between the loess in Jingyang city of Shanxi province [28] and the loess in Lanzhou city of Gansu province, China [13]. In addition, according to the definition for loess type proposed by Gibbs and Holland [29] as shown in the figure, the loess in this study is defined as silty loess.

The compaction curves are illustrated in Figure 5, based on the results of standard Proctor compaction test. The maximum dry densities of the loess and LAT are 1.88 mg/m^3 and 1.53 mg/m^3, respectively. The corresponding optimum moisture contents are 15.4% and 26.0%. Both of the two soils are classified as lean clay (CL) according to the Unified Soil Classification System proposed by ASTM (ASTM, 2017) [27]. Quartz, montmorillonite, feldspar, calcite, and magnetite could be found in the loess soil according to the results of X-ray diffraction (XRD). Only quartz and clay minerals, kaolinite, illite, and montmorillonite could be found in the LAT soil. The mineralogical composition of loess and LAT is illustrated in Figures 6 and 7, respectively. The chemical compositions of the two soils were measured by X-ray fluorescence (XRF), and the major chemical oxides are listed in Table 2.

3. Test Schedule and Method

Falling-head permeability tests were carried out on the pure loess (PL) and the lateritic soil (LAT) with various dry densities to obtain the basic permeability characteristics of the two geomaterials. On the basis of the results of the standard Proctor compaction tests, various dry densities of soil samples were predetermined (as shown in Table 3). To ensure consistency, each sample was compacted inside a metal cylinder (diameter × height = 61.8 × 40 mm) in five layers, with the top of each layer having been scored in a random pattern. The saturation process was performed immediately after compaction and then followed by the permeability tests. The test details are listed in Table 3.

To investigate the effect of lime content on the saturated permeability characteristics of loess with different densities, falling-head tests were also performed on lime-treated loess (LTL samples). The analytical-reagent $Ca(OH)^2$ by weight was mixed into the pure loess; then the mixed soil was wet-compacted inside a metal cylinder, the same as the PL and LAT samples. After compaction, the LTL samples were wrapped in plastic bags and left in a curing box for 28 days at 20°C and 90% relative humidity. After curing, the specimens were saturated by the vacuum saturation method and prepared for the falling-head permeability test. The test details are shown in Table 4. The void ratio before test e was different from the void ratio after compaction e_0 for LTL sample, because during curing period the chemical reaction $Ca(OH)^2 + CO_2$ (from the air) $= CaCO_3 + H_2O$ would happen. The void ratio after compaction e_0 was

Figure 1: Location A of the loess sample in Qingyang, China.

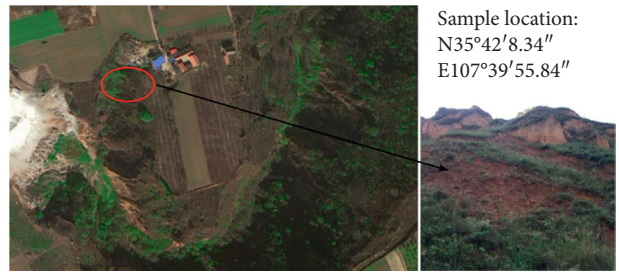

Figure 2: Location of the LAT soil sample in Qingyang, China.

Table 1: Physical properties of loess and LAT soil in this study.

Soil type	Contents of fraction (%)			G_s	Liquid limit (%)	Plastic limit (%)	Plastic index	USCS
	Sand	Silt	Clay					
Loess	3.8	95.4	0.8	2.70	34	22	12	CL
LAT	0	81.5	18.5	2.56	48	28	20	CL

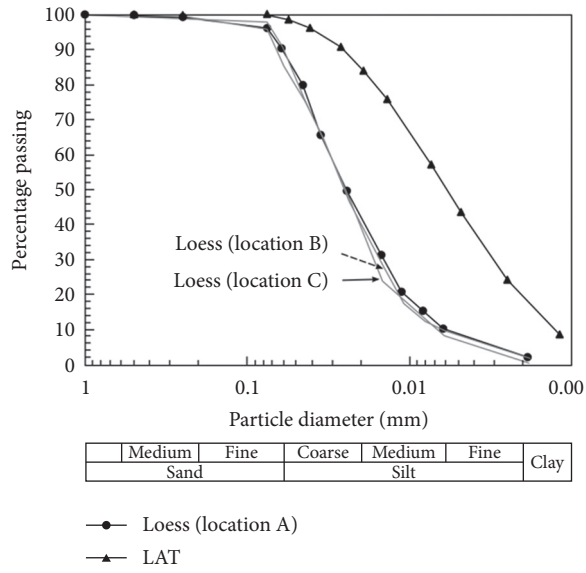

Figure 3: Particle size distribution curves.

calculated by $(V - ((m_{\text{loess}}/G_{\text{sloess}}) - (m_{\text{Ca(OH)}_2}/G_{s\text{Ca(OH)}_2})))/((m_{\text{loess}}/G_{\text{sloess}}) + (m_{\text{Ca(OH)}_2}/G_{s\text{Ca(OH)}_2}))$, where V is the total volume of the specimen, m loess and $m_{\text{Ca(OH)}_2}$ are the dry mass of loess and Ca(OH)_2, and G loess and $G_{s\text{Ca(OH)}_2}$ are the specific gravity. Assuming+ that Ca(OH)_2 in sample was completely changed to CaCO_3 after 28-day curing in this study, the void ratio before test of LTL can be calculated as $(V - ((m_{\text{loess}}/G_{\text{sloess}}) - (m_{\text{Ca(OH)}_2}/G_{s\text{Ca(OH)}_2})))/$

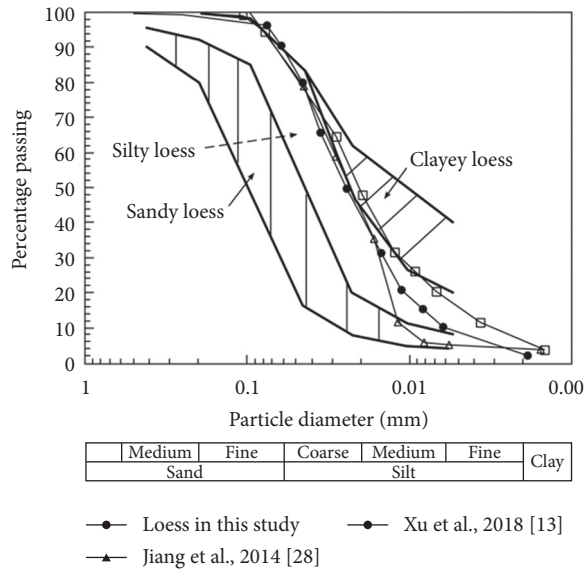

Figure 4: PSD curves of other loess soils in the loess and LAT in previous studies for comparison.

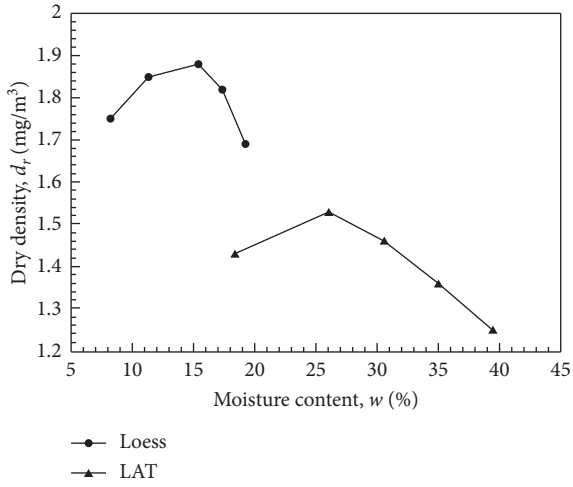

Figure 5: Compaction curves of the loess and LAT.

$((m_{\text{loess}}/G_{\text{sloess}}) + (m_{\text{Ca(OH)}_2}/G_{s\text{Ca(OH)}_2}))$, where m_{CaCO_3} is the dry mass of $CaCO_3$ and $G_{s\text{CaCO}_3}$ is the specific gravity.

The LAT soil, a local geomaterial distributed on the loess plateau whose area is 640, 000 square kilometers in northwestern China, would be more economical and environmental than the lime as for loess treatment, if it can also improve the antipermeability. Loess soils were mixed with different contents of LAT and lime content of 3% before compaction (MLTL samples). After the saturation process and curing period, the falling-head tests were carried out. 3% was optimum content for lime treatment only, revealed by the results of LTL samples, as it will be mentioned in the chapter of test result. The test details are shown in Table 5.

In the local area, people used to cover the sunken loess ground with high density LAT to make the rainwater be stored. In this study, to find out the influence of the coverage of high density LAT on k_{sat} of the pure loess, the falling-head permeability tests of different thickness of LAT coverage were carried out (CL samples). The test sample consisted of two layers; the upper layer was the LAT and the bottom layer was the loess. The dry density of the LAT layer was 1.53 mg/m^3, which is the maximum dry density obtained from the standard Proctor compaction test (Figure 5) and that of the loess layer was 1.40 mg/m^3 which is similar to that of the natural loess. The height of these two-layer samples was 40 mm, which means that increasing LAT coverage's thickness would result in decreased loess soil layer. In

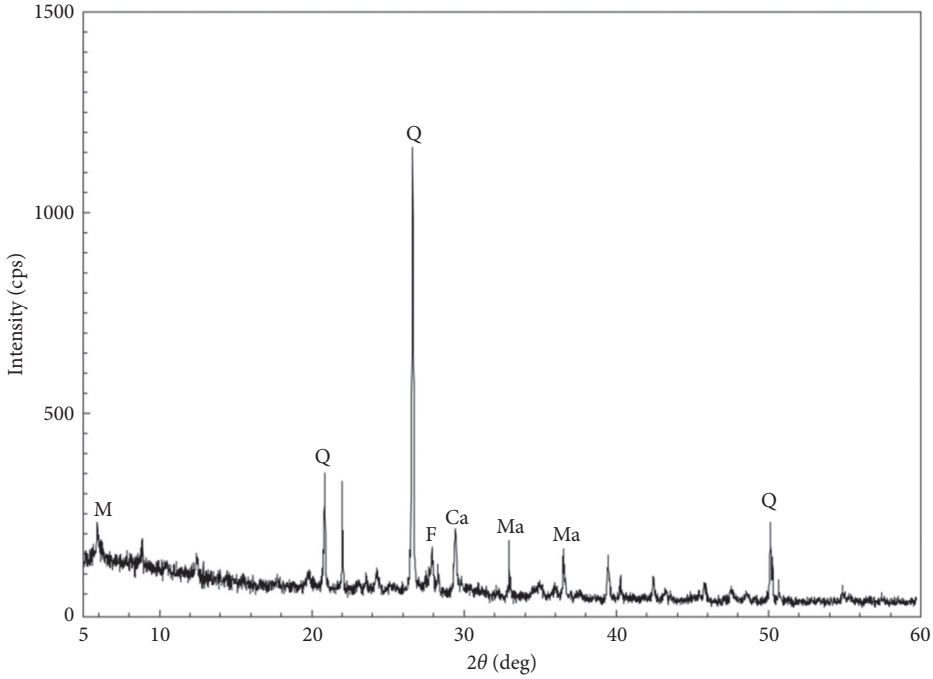

M: montmorillonite
Q: quartz
F: feldspar
Ca: calcite
Ma: magnetite

Figure 6: Mineralogical composition of loess.

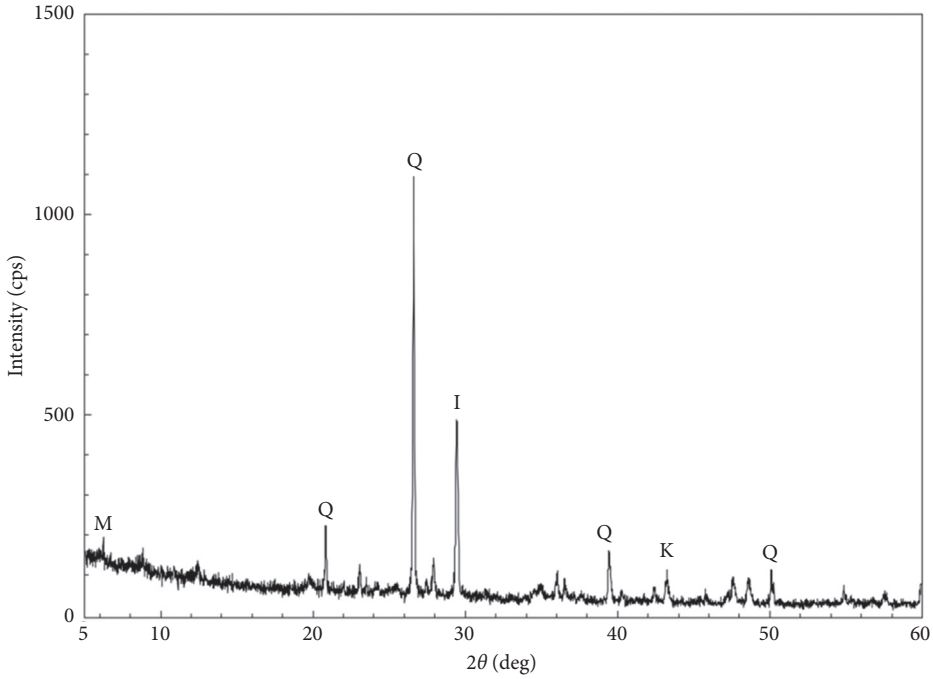

M: montmorillonite
Q: quartz
I: illite
K: kaolinite

Figure 7: Mineralogical composition of LAT.

Table 2: Major chemical oxides presented in the loess and LAT.

Oxide	Loess (%)	LAT (%)
Fe_2O_3	27.4	7.2
Al_2O_3	4.8	14.5
SiO_2	30.4	47.7
CaO	27.3	22.5
K_2O	5.9	3.0

Table 3: Test details of the PL and LAT samples.

Specimen identification	Dry density, d_r (mg/m^3)	Relative compaction degree (%)	Void ratio before test, e	Saturated hydraulic conductivity, k_{sat} (m/s)
PL-01	1.5	80	0.800	6.47×10^{-6}
PL-02	1.55	82	0.742	2.02×10^{-6}
PL-03	1.6	85	0.688	1.00×10^{-6}
PL-04	1.65	88	0.636	7.72×10^{-7}
PL-05	1.7	90	0.588	3.09×10^{-7}
PL-06	1.75	93	0.543	1.79×10^{-7}
PL-07	1.8	96	0.500	4.41×10^{-8}
LAT-08	1.41	92	0.961	5.85×10^{-8}
LAT-09	1.45	95	0.899	2.60×10^{-8}
LAT-10	1.5	98	0.841	3.32×10^{-9}
LAT-11	1.53	100	0.804	1.51×10^{-9}

Table 4: Test details of the LTL samples.

Specimen identification	$Ca(OH)_2$ (%)[a]	Dry density, d_r (mg/m^3)	Void ratio after compaction, e_0	Void ratio before test, e	Saturated hydraulic conductivity, k_{sat} (m/s)
LTL-12	3	1.5	0.789	0.787	2.48×10^{-6}
LTL-13	3	1.55	0.732	0.730	9.63×10^{-7}
LTL-14	3	1.6	0.677	0.676	5.11×10^{-7}
LTL-15	3	1.65	0.627	0.625	2.61×10^{-7}
LTL-16	3	1.7	0.579	0.577	8.96×10^{-8}
LTL-17	3	1.75	0.534	0.532	8.79×10^{-9}
LTL-18	6	1.45	0.841	0.837	3.30×10^{-6}
LTL-19	6	1.5	0.779	0.775	1.50×10^{-6}
LTL-20	6	1.55	0.722	0.718	7.19×10^{-7}
LTL-21	6	1.6	0.668	0.664	2.56×10^{-7}
LTL-22	6	1.65	0.618	0.614	1.08×10^{-7}
LTL-23	6	1.7	0.570	0.567	2.88×10^{-8}
LTL-24	6	1.75	0.525	0.522	9.68×10^{-9}
LTL-25	12	1.4	0.887	0.879	2.90×10^{-6}
LTL-26	12	1.45	0.822	0.814	2.52×10^{-6}
LTL-27	12	1.5	0.761	0.754	1.17×10^{-6}
LTL-28	12	1.55	0.704	0.697	5.80×10^{-7}
LTL-29	12	1.6	0.651	0.644	2.04×10^{-7}
LTL-30	12	1.65	0.601	0.595	7.20×10^{-8}
LTL-31	12	1.7	0.554	0.548	3.80×10^{-8}

[a]Percent by weight.

addition, because the dry density of LAT coverage is higher than that of the loess layer, the density of the whole sample increases with the increasing LAT thickness. The test details are listed in Table 6.

4. Test Result and Discussion

4.1. PL and LAT Soils. The results of the falling-head permeability tests on PL and LAT samples are shown in Figure 8, on a semilogarithmic scale. For both PL and LAT samples, the decreasing void ratio (e) results in decreased saturated hydraulic conductivity (k_{sat}). In other words, the higher relative compaction degree results in the higher antipermeability for each soil. Linear fitting was adopted to describe the relationship of k_{sat} and e, and the equations are listed as follows.

For the PL soils,

$$k_{sat} = 9.5\times10^{-12}\exp(17.2e), \quad R^2 = 0.95, \tag{1a}$$

or

Table 5: Test details of the MLTL samples.

Specimen identification	LAT (%)[b]	Dry density, d_r (mg/m^3)	Void ratio after compaction, e_0	Void ratio before test, e	Saturated hydraulic conductivity, k_{sat} (m/s)
MLTL-32[a]	1	1.52	0.772	0.770	1.01×10^{-6}
MLTL-33	1	1.57	0.715	0.713	1.41×10^{-7}
MLTL-34	1	1.62	0.661	0.659	8.31×10^{-8}
MLTL-35	1	1.67	0.611	0.609	3.40×10^{-8}
MLTL-36	1	1.72	0.564	0.562	1.14×10^{-8}
MLTL-37	1	1.77	0.519	0.517	4.10×10^{-9}
MLTL-38	3	1.55	0.739	0.737	2.95×10^{-7}
MLTL-39	3	1.60	0.682	0.681	1.09×10^{-7}
MLTL-40	3	1.65	0.630	0.628	2.73×10^{-8}
MLTL-41	3	1.70	0.581	0.579	2.10×10^{-8}
MLTL-42	3	1.75	0.534	0.532	6.40×10^{-9}
MLTL-43	3	1.80	0.490	0.489	4.20×10^{-9}
MLTL-44	5	1.58	0.706	0.704	1.29×10^{-7}
MLTL-45	5	1.63	0.651	0.649	5.71×10^{-8}
MLTL-46	5	1.68	0.600	0.598	1.32×10^{-8}
MLTL-47	5	1.73	0.551	0.550	1.47×10^{-8}
MLTL-48	5	1.79	0.506	0.504	5.60×10^{-9}
MLTL-49	5	1.84	0.463	0.461	2.20×10^{-9}
MLTL-50	7	1.61	0.675	0.673	6.83×10^{-8}
MLTL-51	7	1.66	0.621	0.619	2.18×10^{-8}
MLTL-52	7	1.71	0.571	0.569	1.14×10^{-8}
MLTL-53	7	1.77	0.523	0.521	5.29×10^{-9}
MLTL-54	7	1.82	0.478	0.477	3.30×10^{-9}
MLTL-55	9	1.64	0.645	0.644	8.79×10^{-8}
MLTL-56	9	1.69	0.592	0.591	3.12×10^{-8}
MLTL-57	9	1.74	0.542	0.541	9.36×10^{-9}
MLTL-58	9	1.80	0.496	0.494	4.30×10^{-9}
MLTL-59	9	1.85	0.452	0.450	2.30×10^{-9}

[a]All the MLTL samples had the lime content of 3%; [b]percent by weight.

Table 6: Test details of the CL samples.

Specimen identification	LAT (mm)[a]	Dry density[b], d_r (mg/m^3)	Void ratio before test[c], e	Saturated hydraulic conductivity, k_{sat} (m/s)
CL-60	0	1.40	0.929	3.80×10^{-5}
CL-61	10	1.43	0.896	1.01×10^{-6}
CL-62	20	1.46	0.864	1.85×10^{-7}
CL-63	30	1.50	0.834	3.40×10^{-8}

[a]Thickness of LAT layer; [b]dry density of the whole sample; [c]void ratio of the whole sample.

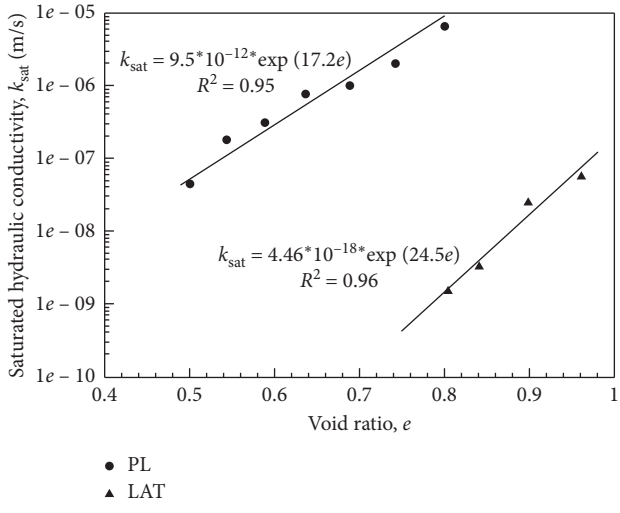

Figure 8: Test data and best-fitting relationships of k_{sat} versus e of PL and LAT samples.

$$\ln k_{sat} = -2.5380 + 17.2e. \quad (1b)$$

For the LAT soils,

$$k_{sat} = 4.46 \times 10^{-18} \exp(24.5e), \quad R^2 = 0.96, \quad (2a)$$

or

$$\ln k_{sat} = -39.951 + 24.5e. \quad (2b)$$

The value of gradient of each soil is different, which means that the two fitting lines are not parallel. The intercepts (k_{sat} at $e = 0$) are 9.5×10^{-12} and 4.46×10^{-18} m/s for the PL and LAT, respectively. Because of the difference between the maximum dry densities of PL and LAT soils, the scopes of void ratio of the two soil samples (predetermined as shown in Table 3) are not overlapped. However, through the fitting lines as seen in the figure, k_{sat} of LAT is obviously lower than that of PL soil with similar void ratio. The antipermeability of LAT is better than that of PL with the same void ratio in engineering practice. It may be because the content of the clay fraction of LAT is higher than that of PL (Table 1), the clay particles would fill in the void space among the silt particles in the LAT soil, and that would result in lower k_{sat} as compared with PL soil.

4.2. LTL Soils. The results of the LTL samples are illustrated in Figure 9. For comparison, the results of the PL samples with its best-fitting line, of which the lime content could be treated as zero, are shown together in the figure. It can be seen that, for each lime content, k_{sat} decreases with the decreasing e, as to be expected. For the LTL samples with 3% lime content, a fitting line which is parallel to the PL line in (1a) can be recognized, which is expressed as

$$k_{sat} = 3.8 \times 10^{-12} \exp(17.2e), \quad R^2 = 0.96, \quad (3a)$$

or

$$\ln k_{sat} = -26.296 + 17.2e. \quad (3b)$$

For the LTL samples with 6% and 12% lime content, separated lines for each cannot be identified. The data points are distributed around a line that can be expressed as in the following equations, although there are few scatterings at high void ratios:

$$k_{sat} = 2.62 \times 10^{-12} \exp(17.2e), \quad R^2 = 0.94, \quad (4a)$$

$$\ln k_{sat} = -26.668 + 17.2e. \quad (4b)$$

The value of gradient of each line is identical, despite the different lime contents, but the intercept seems to be dominated by the lime content. Figure 10 shows the test data of the intercepts and the corresponding lime contents of each line in Figure 9. As seen in Figure 10, with the increasing lime content, the intercept decreases gradually. As the lime content changes from 0% to 3%, the rate of intercept decrease is 60%, and the rate of that from 3% to 6% is 31%. When the lime content changes from 6% to 12%, there is no dramatic influence of the increasing lime content on k_{sat} (Figure 9), and the intercepts of 6% and 12% are assumed to be identical as in (4a). Thus, the lime content of 3% might be the most economical and environmental (not the most effective) as for lime treatment only; a little addition of lime could obtain a considerable antipermeability.

Further, in order to get the value of intercept of the soil with lime content out of the tested scope, linear lines are drawn between the adjacent data points as shown in Figure 10, and the equations are listed together. Thus, for any LTL soils encountered in construction, the linear relationship between its k_{sat} and e in the semilogarithmic scale similar to the lines in Figure 9 could be obtained, by getting the intercept in Figure 10 as the lime content known, with the value of slope which is constant (Figure 9). This empirical algorithm would be very helpful for engineering design and numerical simulation in the large-scope area in which the loess studied is widely distributed with high homogeneity.

4.3. MLTL and CL Soils. The lime content of 3% was verified to be the most economical and environmental for lime treatment, and, to find out if the local geomaterial, lateritic soil (LAT), could partially replace lime for antipermeability, different contents of LAT were mixed into the loess soil with lime content of 3% (MLTL samples) before compaction. The test results of the MLTL samples are illustrated in Figure 11, with test data of LTL samples with 3% lime content and the linear lines together for comparison.

As to be expected, for all LAT contents, k_{sat} of the MLTL samples decreases with the decreasing e. k_{sat}-e curves of MLTL samples of all LAT contents are crossed by each other, which are not shown in Figure 11 for clarity. Instead, a single linear line which is parallel with the fitting lines of LTL samples could be recognized based on the data of all MLTL samples, as illustrated in Figure 11. The intercept of MLTL line is 0.8×10^{-12} m/s, lower than that of the lines of PL and LTL samples. The addition of LAT could obviously decrease k_{sat} of the LTL soils with 3% lime, even much lower than that of the LTL soils with 6% and 12% lime. However, for the scope of LAT contents studied here (1%–9%), the influence of different contents on k_{sat} is not found. No matter the LAT contents that the MLTL samples have, the data points lay nearby the only one linear line as mentioned above; k_{sat} is only affected by the void ratio. For the LTL soils with different lime contents, it can be seen in the mini figure in Figure 11 that the intercept of fitting line decreases gradually with the increasing lime content of 0% (pure loess) to 12%. However, as to the MLTL samples, a gradual tendency could not be found in this study; the intercept shows an

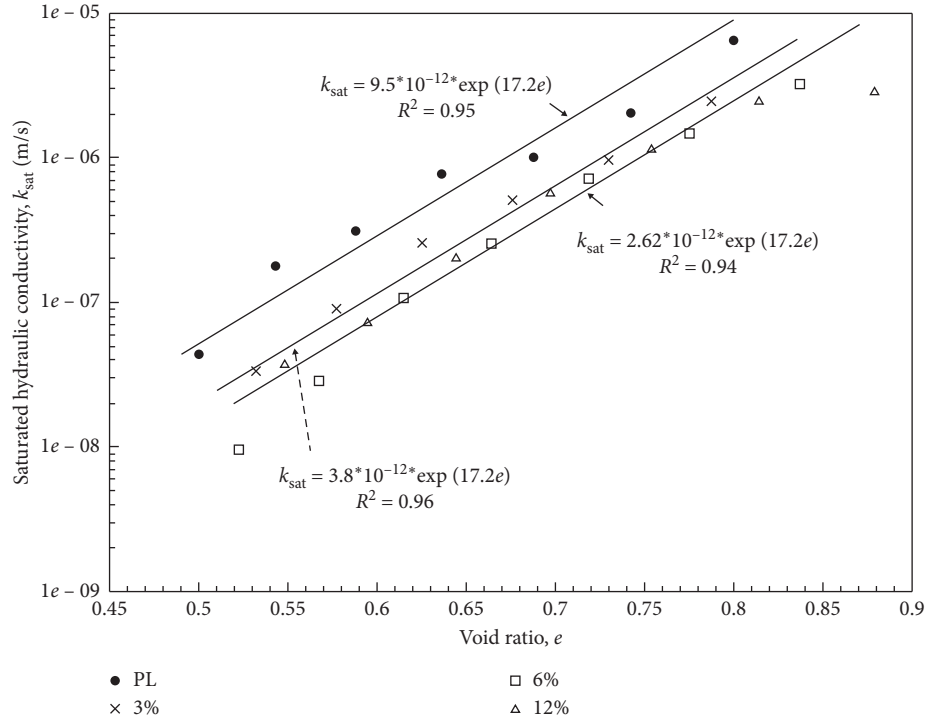

Figure 9: Test data and best-fitting relationships of k_{sat} versus e of LTL samples with different lime contents.

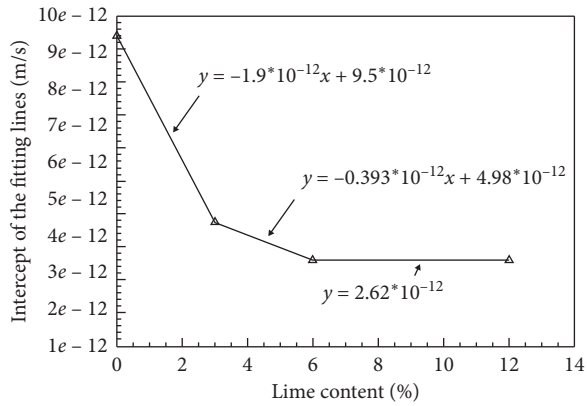

Figure 10: Relationship between the intercept and lime content of the linear fitting lines of lime-treated loess.

abrupt drop for the LAT content changes from 0% (LTL with 3% lime) to 1%. This may be because the micropores decreased very slightly with the increasing LAT contents at that content higher than 1%. Generally, k_{sat} is dominated by the micropores in soil [18, 30]. Thus, as the LAT content increased from 1% to 9%, it seems that the LAT content did not affect k_{sat} dramatically and the soil density (void ratio) was dominated.

k_{sat} of the MLTL soils with 0% to 1% LAT will be the emphasis in the further work.

The test data of k_{sat} versus e of the CL samples (pure loess covered by the high density LAT) are shown in Figure 12, and the relationship of the thickness and k_{sat} is shown in Figure 13. When the thickness of coverage was zero (CL-60), the sample was pure loess with dry density of 1.40 mg/m^3, which is similar to that of natural loess, and the data point locates a little below the PL line. As the thickness of LAT increases, k_{sat} decreases and the fitting linear line trends to the LAT line. If the thickness of the LAT coverage is infinite, the relationship of k_{sat} and e would be the LAT line. The high density LAT coverage could obviously decrease k_{sat}. k_{sat} of the CL sample with 30 mm LAT is 3.40×10^{-8} m/s, lower than k_{sat} of the PL sample with dry density of 1.80 g/cm^3 (corresponding $e = 0.500$), of which the relative compaction degree is 0.96 (Table 3). It reveals that, in engineering practice, the coverage at least 30 mm of LAT is very useful for improving the antipermeability, as compared to the treatment of compacting the pure loess to a high density.

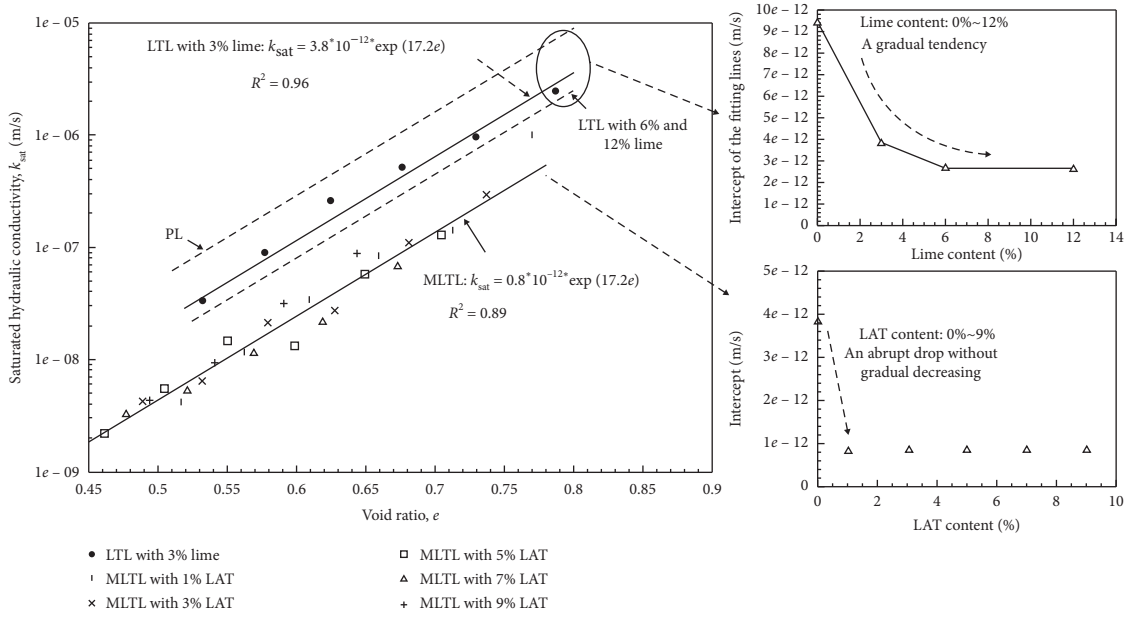

Figure 11: Test data and best-fitting relationships of k_{sat} versus e of MLTL samples.

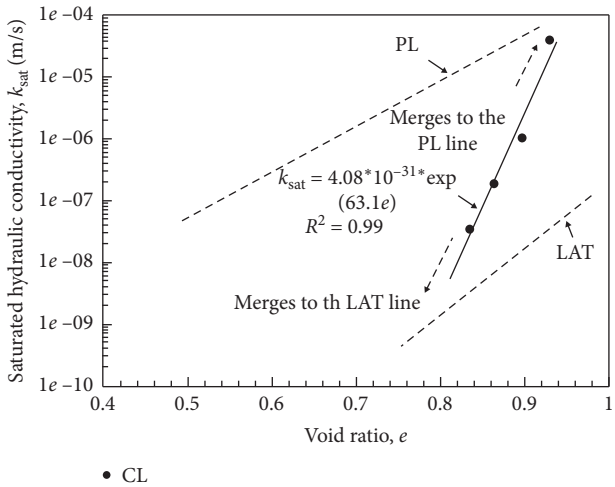

Figure 12: Test data of the CL samples.

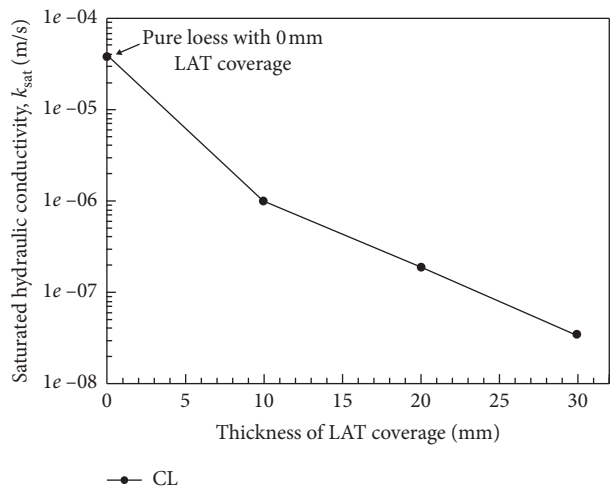

Figure 13: k_{sat} versus LAT coverage.

5. Conclusions

A series of falling-head permeability tests were carried out on the pure loess (PL), lateritic soil (LAT), lime-treated loess (LTL), lime-treated loess mixed with LAT, and pure loess covered with high density LAT samples. The test results are analyzed and the following conclusions can be drawn.

(1) The saturated hydraulic conductivity (k_{sat}) of LAT is much lower than that of PL with the same void ratio. It may be because the content of the clay fraction of LAT is higher than that of PL according to the particle size distributions, and the clay particles would fill in the void space among the silt particles in the LAT soil.

(2) The lime treatment could obviously influence k_{sat} of loess, and the increasing lime content results in decreasing k_{sat} with the same void ratio. A group of parallel lines can be used to describe the relationships of k_{sat} and e for the loess with different lime contents on a semilogarithmic scale. The intercept of the linear line is dependent on the value of lime content. 3% of lime content may be the most economical and environmental as for lime treatment only. Besides, an empirical algorithm is proposed for estimating k_{sat} of loess with the lime content which is out of the scope studied in this paper. It would be very helpful for engineering design and numerical simulation for safety evaluation.

(3) The local geomaterial, LAT soil, could partially replace the lime as for improving the antipermeability of loess. A little addition of LAT, e.g., 1% into the loess with 3% lime content, could obviously decrease k_{sat}, even lower than k_{sat} of 12% lime-treated loess.

(4) The coverage of high density LAT on loess, which is the most common treatment for antipermeability used by local people, is verified to be effective. The increasing thickness of LAT coverage could improve the antipermeability, and for engineering practice at least of 30 mm of the coverage is suggested.

Data Availability

The data used to support the findings of this study are included within the article.

Disclosure

This research was performed as part of the employment of the authors; the employer was Guangdong University of Technology.

Conflicts of Interest

The authors declare that there are no conflicts of interest regarding the publication of this paper.

References

[1] D. Haase, J. Fink, G. Haase et al., "Loess in Europe—its spatial distribution based on a European loess map, scale 1 : 2,500,000," *Quaternary Science Reviews*, vol. 26, no. 9-10, pp. 1301–1312, 2007.

[2] D. R. Muhs, "The geochemistry of loess: Asian and north American deposits compared," *Journal of Asian Earth Sciences*, vol. 155, pp. 81–115, 2018.

[3] S. B. Markovic, T. Stevens, G. J. Kukla et al., "Danube loess stratigraphy—towards a pan-European loess stratigraphic model," *Earth Science Reviews*, vol. 148, pp. 228–258, 2015.

[4] R. J. Schaetzl and J. W. Attig, "The loess cover of northeastern Wisconsin," *Quaternary Research*, vol. 79, no. 2, pp. 199–214, 2013.

[5] Z. J. Zhou, S. S. Zhu, X. Kong, J. Lei, and T. Liu, "Optimization analysis of settlement parameters for postgrouting piles in loess area of Shaanxi, China," *Advances in Civil Engineering*, vol. 2019, Article ID 7085104, 16 pages, 2019.

[6] H. B. Xue, F. N. Dang, Y. L. Li, X. Yin, and M. Lei, "Vector sum analysis method of loess slope stability under rising groundwater level conditions," *Advances in Civil Engineering*, vol. 2019, Article ID 9703184, 12 pages, 2019.

[7] V. I. Travush, A. V. Tsoi, and A. T. Marufii, "Influence of local wetting of loess soil on the redistribution of reactive pressures under foundations," *Soil Mechanics and Foundation Engineering*, vol. 53, no. 2, pp. 67–70, 2016.

[8] X. L. Wang, Y. P. Zhu, and X. F. Huang, "Field tests on deformation property of self-weight collapsible loess with large thickness," *International Journal of Geomechanics*, vol. 14, no. 3, Article ID 04014001, 2014.

[9] J. Kozubal and D. Steshenko, "The complex compaction method of an unstable loess substrate," *Arabian Journal of Geosciences*, vol. 8, no. 8, pp. 6189–6198, 2015.

[10] B. X. Yuan, L. Xiong, L. H. Zhai et al., "Transparent synthetic soil and its application in modeling of soil-structure interaction using optical system," *Frontiers in Earth Science*, vol. 7, no. 9, 2019.

[11] J. Kozubal, D. Steshenko, and B. Galay, "The improvement of loess substrates with a new type of soil column with a reliability assessment," *Road Materials and Pavement Design*, vol. 15, no. 4, pp. 856–871, 2014.

[12] L. Z. Wu, Y. Zhou, P. Sun, J. S. Shi, G. G. Liu, and L. Y. Bai, "Laboratory characterization of rainfall-induced loess slope failure," *CATENA*, vol. 150, pp. 1–8, 2017.

[13] Y. Xu, C. F. Leung, J. Yu, and W. Chen, "Numerical modelling of hydro-mechanical behaviour of ground settlement due to rising water table in loess," *Natural Hazards*, vol. 94, no. 1, pp. 241–260, 2018.

[14] H. W. Ma and Q. Ma, "Experimental studies on the mechanical properties of loess stabilized with sodium carboxymethyl cellulose," *Advances in Materials Science and Engineering*, vol. 2019, Article ID 9375685, 8 pages, 2019.

[15] W. Liu, J. Wang, G. C. Lin, L. Wen, and Q. Wang, "Microscopic mechanism affecting shear strength in lignin-treated loess samples," *Advances in Materials Science and Engineering*, vol. 2019, Article ID 7126040, 12 pages, 2019.

[16] Y. X. Wang, P. P. Guo, W. X. Ren et al., "Laboratory investigation on strength characteristics of expansive soil treated with jute fiber reinforcement," *International Journal of Geomechanics*, vol. 17, p. 12, Article ID 04017101, 2017.

[17] B. X. Yuan, M. Sun, Y. X. Wang et al., "Full 3D displacement measuring system for 3D displacement field of soil around a

laterally loaded pile in transparent soil," *International Journal of Geomechanics*, vol. 19, p. 8, Article ID 04019028, 2019.

[18] Z. Metelková, J. Boháč, R. Přikryl, and I. Sedlářová, "Maturation of loess treated with variable lime admixture: pore space textural evolution and related phase changes," *Applied Clay Science*, vol. 61, pp. 37–43, 2012.

[19] S.-l. Wang, Q.-f. Lv, H. Baaj, X.-y. Li, and Y.-x. Zhao, "Volume change behaviour and microstructure of stabilized loess under cyclic freeze-thaw conditions," *Canadian Journal of Civil Engineering*, vol. 43, no. 10, pp. 865–874, 2016.

[20] B.-h. Yang, X.-z. Weng, J.-z. Liu et al., "Strength characteristics of modified polypropylene fiber and cement-reinforced loess," *Journal of Central South University Journal of Central South University*, vol. 24, no. 3, pp. 560–568, 2017.

[21] J.-D. Wang, P. Li, Y. Ma, S. K. Vanapalli, and X.-G. Wang, "Change in pore-size distribution of collapsible loess due to loading and inundating," *Acta Geotechnica*, vol. 15, no. 5, pp. 1081–1094, 2019.

[22] Y. Y. Gao, H. Qian, X. Y. Li, J. Chen, and H. Jia, "Effects of lime treatment on the hydraulic conductivity and microstructure of loess," *Environmental Earth Sciences*, vol. 77, p. 15, Article ID 529, 2018.

[23] H. Gao and M. Shao, "Effects of temperature changes on soil hydraulic properties," *Soil and Tillage Research*, vol. 153, pp. 145–154, 2015.

[24] W. Hu, M. A. Shao, and B. C. Si, "Seasonal changes in surface bulk density and saturated hydraulic conductivity of natural landscapes," *European Journal of Soil Science*, vol. 63, no. 6, pp. 820–830, 2012.

[25] K. Ezziane, E. H. Kadri, and R. Siddique, "Investigation of slag cement quality through the analysis of its efficiency coefficient," *European Journal of Environmental and Civil Engineering*, vol. 15, no. 10, pp. 1393–1411, 2011.

[26] F. Faleschini, P. De Marzi, and C. Pellegrino, "Recycled concrete containing EAF slag: environmental assessment through LCA," *European Journal of Environmental and Civil Engineering*, vol. 18, no. 9, pp. 1009–1024, 2014.

[27] American Society for Testing and Materials (ASTM), "Standard practice for classification of soils for engineering purposes (unified soil classification system)," ASTM, West Conshohocken, PA, USA, D2487-17, 2017.

[28] M. Jiang, F. Zhang, H. Hu, Y. Cui, and J. Peng, "Structural characterization of natural loess and remolded loess under triaxial tests," *Engineering Geology*, vol. 181, pp. 249–260, 2014.

[29] H. J. Gibbs and W. Y. Holland, "Petrographic and engineering properties of loess," *Engineering Monograph*, vol. 25, no. 5, pp. 1–37, 1961.

[30] X. Xie, P. Li, X. K. Hou et al., "Microstructure of compacted loess and its influence on the soil-water characteristic curve," *Advances in Materials Science and Engineering*, vol. 2020, Article ID 3402607, 12 pages, 2020.